BIOCHEMISTRY
including biophysical chemistry & molecular biology

Article

pubs.acs.org/biochemistry

Calcium Ion Binding Properties of *Medicago truncatula* Calcium/Calmodulin-Dependent Protein Kinase

David J. K. Swainsbury,[†] Liang Zhou,[†] Giles E. D. Oldroyd,[‡] and Stephen Bornemann*[,†]

[†]Department of Biological Chemistry, John Innes Centre, Norwich Research Park, Norwich NR4 7UH, United Kingdom
[‡]Department of Cell and Developmental Biology, John Innes Centre, Norwich Research Park, Norwich NR4 7UH, United Kingdom

Supporting Information

ABSTRACT: A calcium/calmodulin-dependent protein kinase (CCaMK) is essential in the interpretation of calcium oscillations in plant root cells for the establishment of symbiotic relationships with rhizobia and mycorrhizal fungi. Some of its properties have been studied in detail, but its calcium ion binding properties and subsequent conformational change have not. A biophysical approach was taken with constructs comprising either the visinin-like domain of *Medicago truncatula* CCaMK, which contains EF-hand motifs, or this domain together with the autoinhibitory domain. The visinin-like domain binds three calcium ions, leading to a conformational change involving the exposure of hydrophobic surfaces and a change in tertiary but not net secondary or quaternary structure. The affinity for calcium ions of visinin-like domain EF-hands 1 and 2 (K_d = 200 ± 50 nM) was appropriate for the interpretation of calcium oscillations (~125−850 nM), while that of EF-hand 3 (K_d ≤ 20 nM) implied occupancy at basal calcium ion levels. Calcium dissociation rate constants were determined for the visinin-like domain of CCaMK, *M. truncatula* calmodulin 1, and the complex between these two proteins (the slowest of which was 0.123 ± 0.002 s^{-1}), suggesting the corresponding calcium association rate constants were at or near the diffusion-limited rate. In addition, the dissociation of calmodulin from the protein complex was shown to be on the same time scale as the dissociation of calcium ions. These observations suggest that the formation and dissociation of the complex between calmodulin and CCaMK would substantially mirror calcium oscillations, which typically have a 90 s periodicity.

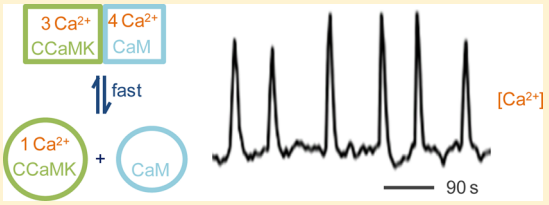

The majority of land plants form an ancient symbiotic association with arbuscular mycorrhizal fungi that facilitates the uptake of water, phosphate, and other nutrients.[1] Legumes also form a symbiotic relationship with rhizobia, allowing them to fix nitrogen from the atmosphere.[2] The latter symbiosis appears to have evolved from the former because the distinct developmental changes in the plant root required for each symbiotic relationship to become established involve many common elements in their signaling pathways. Central to the common symbiosis pathway is the occurrence of calcium spiking, whereby the intracellular calcium ion concentration oscillates in response to nodulation or mycorrhization factors secreted by the respective microbial symbionts.[3,4] A calcium/calmodulin protein kinase (CCaMK) has been shown genetically to be downstream of calcium spiking[5] and to be essential for both symbiotic relationships.[6,7] The immediate output of CCaMK appears to be the phosphorylation of downstream targets, such as CYCLOPS,[8] and both loss and gain of function mutants of *CCaMK* have been reported.[6,9,10] Thus, CCaMK appears to be responsible for the interpretation of calcium spiking.

CCaMK was first identified in lily.[11] It comprises an N-terminal kinase domain (Figure 1), a central autoinhibitory domain (AID), which is capable of binding calmodulin (CaM), and a C-terminal visinin-like domain (VLD),[12] which contains EF-hand motifs associated with the binding of calcium ions. Experiments in vitro have shown that the binding of calcium ions stimulates autophosphorylation of Thr267 in lily CCaMK.[13] CCaMK also binds CaM in a calcium ion-dependent manner,[11] and autophosphorylation enhances the affinity between these two proteins.[14] Interestingly, the binding of CaM also inhibits autophosphorylation.[13] The phosphorylation of targets by CCaMK is dependent on both calcium ions and CaM, and the maximal activity is enhanced by autophosphorylation.[13] CCaMK from *Zea mays* has properties similar to those of the lily protein except that CaM does not inhibit autophosphorylation and that autophosphorylation gave calcium ion-independent target phosphorylation.[15]

The VLD of CCaMK appears to be unique among protein kinases. Deletion of some or all of the EF-hands of this domain in lily CCaMK removes the stimulation of autophosphorylation by calcium ions[13,14] without abolishing the binding of CaM.[12] By contrast, deletion of successive EF-hands leads to a gradual loss of target phosphorylation activity, which decreases to 4% of the wild-type activity.[12] Point mutations in the EF-hands of *Lotus japonicas* CCaMK abolish the accommodation of rhizobia in nodules and adversely affect mycorrhization.[16] Therefore, the

Received: June 20, 2012
Revised: August 8, 2012
Published: August 13, 2012

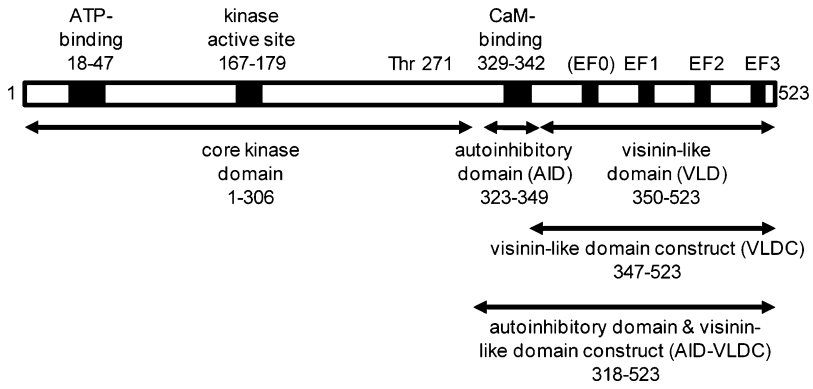

Figure 1. Domains, motifs, and constructs of CCaMK. Features of CCaMK are indicated with numbers relating to the primary sequence of the *Medicago truncatula* protein. The motif of EF-hand 0 is poorly conserved (Table 2).

VLD appears to be essential for the correct interpretation of calcium spiking.

This study focuses on how tightly the VLD of *Medicago truncatula* CCaMK binds calcium ions and the time scale on which it occurs together with the nature of any associated protein conformational change in the context of calcium spiking.

MATERIALS AND METHODS

Expression and Purification of Proteins. The gene for *M. truncatula* CCaMK was synthesized (Figure S1 of the Supporting Information) with optimal codon usage for *Escherichia coli* expression (Genscript). It was used as a template to generate an AID and VLD construct (AID-VLDC; CCaMK residues 318−523) without a tag and a VLD construct (VLDC; CCaMK residues 347−523) with an N-terminal His_6 tag using the pET101/D-TOPO kit (Invitrogen). The forward primers for the AID-VLDC and VLDC were 5′-*CAC*CATGCCGGAAATTGTGTCTCGC and 5′-*CACC*ATG**CATCACCATCACCATCAC**TTCCTGCGCACCAAAAAAC (directional cloning overhang in italics, start codon underlined, and tag sequence in bold), respectively, and the reverse primer for both was 5′-*CTA*CGGGCGGATTGACGACAGA (reverse complement stop codon in italics). Site-directed mutations of the EF-hands of the VLDC were generated using the QuikChange Lightning site-directed mutagenesis kit (Stratagene). The invariant Asp residue (corresponding to the first residue of the motif and ligand X to a bound calcium ion[17]) in each of EF-hands 1−3 was mutated to Ala to abolish the ability to bind calcium ions (residues 413, 449, and 491 in the context of the full-length CCaMK sequence, respectively). The forward primers for mutating EF-hands 1−3 were 5′-CGCATTTTCGATCTGTTCGCTAATAATCGCGACGGT, 5′-TGCTTTCAAATGTATGCTACCGACCGTTCGGGTTGC, and 5′-GAAATTTTCGATCTGATGGCTGCCAACAATGATGGC (mutated base underlined), respectively. All constructs were verified by sequencing.

The AID-VLDC was expressed in *E. coli* BL21 Star(DE3) cells grown in autoinduction medium (Formedium) at 37 °C for 2 h[18] followed by 20 °C for 20 h. Cells were harvested at 5000*g* for 20 min at 4 °C, resuspended in 50 mM Tris-HCl (pH 7.5) containing 1 M NaCl, 1 mM $CaCl_2$, 1 mM DTT, DNase I, and cOmplete ULTRA EDTA-free protease inhibitor cocktail tablets (Roche), and disrupted with a TS Series Benchtop 1.1 kW cell disruptor (Constant Systems Ltd.) at 25K psi. The cell lysate was centrifuged at 20000*g* for 30 min at 4 °C, and the supernatant was loaded onto a 10 mL Calmodulin Sepharose 4B column (GE Healthcare) that was previously equilibrated with 50 mM Tris-HCl (pH 7.5) containing 1 M NaCl, 2 mM $CaCl_2$, and 1 mM DTT. After being washed with 5.5 column volumes of the same buffer, the protein was eluted with 50 mM Tris-HCl (pH 7.5) containing 2 mM EDTA and 1 mM DTT. The protein was further purified using a HiLoad 16/600 Superdex 75 gel filtration column (GE Healthcare), previously equilibrated with 50 mM Tris-HCl (pH 7.5) containing 100 mM NaCl and 1 mM DTT. The protein concentration was determined by the absorbance at 280 nm using a predicted extinction coefficient of 9970 M^{-1} cm^{-1}.[19]

The VLDC was expressed, and cells were harvested as described above for the AID-VLDC except that cells were resuspended in 50 mM Tris-HCl (pH 7.5) containing 300 mM NaCl, 10 mM imadazole, DNase I, and cOmplete ULTRA EDTA-free protease inhibitor cocktail tablets (Roche). The cell free extract was applied to a 1 mL HisTrap FF column (GE healthcare) that was previously equilibrated with 50 mM Tris-HCl (pH 7.5) containing 300 mM NaCl and 10 mM imidazole. After application of a further 5 column volumes of this buffer, the protein was eluted with 50 mM Tris-HCl (pH 7.5) containing 300 mM NaCl and 500 mM imadazole. The protein was further purified using size exclusion chromatography as described above. Because of the lack of Trp residues in the VLDC, a theoretical extinction coefficient may have been unreliable. The protein concentration was therefore determined by absorbance at 280 nm using an extinction coefficient of 4745 M^{-1} cm^{-1} that was defined by reference to amino acid analysis of the VLDC (University of Cambridge Protein and Nucleic Acid Facility, Cambridge, United Kindgom).

The gene for canonical *M. truncatula* CaM 1 (GenBank entry AAM81202.1) was synthesized (Genscript) with optimal codon usage for expression in *E. coli* (Figure S2 of the Supporting Information) and subcloned into pET-21a(+) (Novagen). *E. coli* BL21(DE3)pLysS harboring the resulting expression plasmid was grown at 37 °C in 6 L of LB, and protein expression was induced with the addition of 1 mM isopropyl β-D-1-thiogalactopyranoside when the culture OD at 600 nm reached 0.5. After incubation for a further 3 h, cells were harvested at 5000*g* for 10 min at 4 °C, resuspended in 50 mL of 50 mM Tris-HCl (pH 7.5) containing 1 mM $CaCl_2$, 6 mg/mL DNase I, and a cOmplete ULTRA EDTA-free protease inhibitor cocktail tablet (Roche), and disrupted and centrifuged as described above. The supernatant was heated to 90 °C for 3 min, cooled on ice for 5 min, and centrifuged again. CaM was

dx.doi.org/10.1021/bi300826m | *Biochemistry* 2012, 51, 6895−6907

purified using a Phenyl Sepharose Fast Flow column (GE Healthcare) as described previously[20] with further purification using gel filtration as described above. An experimental extinction coefficient of 2545 M^{-1} cm^{-1} at 280 nm was determined as described above.

The identity of each purified protein was confirmed with tryptic digestion and mass spectrometric fingerprinting using standard procedures.

Analytical Ultracentrifugation. Samples were analyzed using a Beckman (High Wycombe, United Kingdom) Optima XL-I analytical ultracentrifuge equipped with absorbance optics and an An-50 Ti rotor. The measurements were taken at 20 °C in 10 mM HEPES buffer (pH 7.5) containing 50 mM NaCl, 1 mM TCEP, and 2 mM $CaCl_2$. Equilibrium experiments were performed, and absorbance profiles were measured at 280 nm every 4 h until equilibrium had been reached. Five scans were collected per velocity. The partial specific volumes of proteins were calculated from their amino acid sequences using SEDNTERP. Data were analyzed using Ultrascan II[21] using the one-component ideal model. Errors were estimated with the Monte Carlo analysis module with default settings except for "ignore runs with variance above", which was set to 2×10^{-4} (default, 1×10^{-4}).

Mass Spectrometry. The binding of calcium ions to proteins was detected using electrospray ionization mass spectrometry (ESI-MS).[22,23] The VLDC WT and its EF-hand muteins were buffer exchanged 1000-fold into 10 mM ammonium acetate (pH 7.5) using Sartorius 10 kDa Vivaspin devices. Samples of 20 μM protein in 25% acetonitrile containing either 100 μM EDTA or 100 μM calcium acetate were analyzed by ESI-MS in negative ion mode on a Q-TOF 2 mass spectrometer (Waters/Micromass UK). Samples were applied to the mass spectrometer via an electrospray ionization interface with a flow rate of 5 μL/min, a desolvation temperature of 150 °C, a desolvation gas flow of 6.7 L/min, and a capillary spray voltage of 2.3 kV. The cone voltage was set to 65 V and the source temperature to 80 °C. Calibration was performed using an 8 μM myoglobin (Sigma) solution in 50% acetonitrile containing 0.1% NH_4OH. Scans were acquired in the mass range m/z 1000−4000. Data were acquired and processed using MassLynx version 4.1 (Waters). Final spectra were generated by combining a number of scans and applying background removal and a Savitzky−Golay smoothing method.

Spectrofluorimetry. The calcium ion-dependent exposure of hydrophobic surfaces on proteins was monitored using 8-anilino-1-naphthalenesulfonic acid (ANS).[24] Samples comprised 10 mM Tris-HCl (pH 7.5) containing 5 μM protein, 50 mM NaCl, 1 mM TCEP, 15 μM ANS, and either 2 mM $CaCl_2$ with 2 mM EDTA or 5 mM $MgCl_2$ with 2 mM EGTA. Fluorescence emission spectra were recorded between 400 and 650 nm on a PerkinElmer LS 55 fluorescence spectrometer using an excitation wavelength of 380 nm with 10 nm slits.

Tryptophan fluorescence was recorded between 310 and 400 nm using an excitation wavelength of 290 nm. Solutions were buffered with 10 mM Tris-HCl (pH 7.5) containing 50 mM NaCl, 1 mM TCEP, and 2 mM $CaCl_2$. To 0.8 mL of 5 μM AID-VLDC was added 0.2 mL of 50 μM CaM followed by 0.1 mL of 0.25 M EDTA.

Circular Dichroism Spectroscopy. Circular dichroism (CD) spectra were recorded on a Jasco J-710 spectropolarimeter. Samples comprised 10 mM HEPES (pH 7.5) containing 40 μM protein and either 2 mM EDTA, 2 mM $CaCl_2$ or 5 mM $MgCl_2$ with 2 mM EGTA. Near-UV (250−330 nm) and far-UV (180−260 nm) spectra were recorded using 10 and 0.1 mm quartz cuvettes, respectively. Spectra were recorded with a sensitivity of 100 mdeg, a data pitch of 0.2 nm, a response time of 4 s, and a bandwidth of 1.0 nm at a scan speed of 20 nm/min. Quadruplet spectra were averaged followed by the subtraction of buffer only control spectra. Far-UV spectra were smoothed using the Savitzky−Golay method with a factor of 5 using the Jasco CD spectropolarimeter software and analyzed with Dichroweb[25] using the CDSSTR algorithm and reference set 6.[26]

Removal of Calcium Ions from Solutions. For the removal of calcium ions from buffers, a 40 mL Chelex 100 column (Bio-Rad) was treated with 2 column volumes of 1 M HCl followed by 2.5 column volumes of Milli-Q water, 2 column volumes of 1 M Tris-HCl (pH 7.5), and 5 column volumes of Milli-Q water. The sample buffer consisted of 10 mM Tris-HCl (≥99%; Formedium) (pH 7.5) containing 50 mM NaCl (≥99.8%; Sigma) and 1 mM TCEP (≥98%; Sigma) unless stated otherwise. This was passed through the column as a 2-fold concentrate three times before being diluted to the final concentration allowing a final volume of up to 1 L to be prepared. Plasticware that was washed with 1 M HCl and rinsed with Milli-Q water was used throughout this work.

For the removal of calcium ions from either the VLDC or the AID-VLDC solutions, a 1 ml His-Trap FF column (GE Healthcare) was treated with with 2 column volumes of 1 M HCl followed by 5 column volumes of Milli-Q water before being equilibrated with 15 column volumes of buffer. Protein solutions were concentrated to 0.5 mL using a Sartorius Vivaspin 4 mL device with a 10000 molecular weight cutoff that had been prewashed with Milli-Q water. Concentrated samples were passed through the column, and fractions containing protein were pooled, reconcentrated, and passed through the column again. This was repeated to give a total of three column passes.

Calcium ions were removed from CaM solutions in 25 mM Tris-HCl (pH 7.5) containing 50 mM NaCl by treatment with 10 mM EDTA and dialysis against buffer without EDTA followed by three rounds of desalting with PD-10 columns and concentrating with Vivaspin devices. This method was not suitable for either the VLDC or the AID-VLDC because of an inability to remove all of the chelator from these proteins.

Isothermal Titration Calorimetry. Isothermal titration calorimetry (ITC) experiments were conducted using an iTC 200 instrument (Microcal/GE Healthcare) at 25 °C using either the VLDC in 10 mM Tris-HCl buffer (pH 7.5) containing 50 mM NaCl and 1 mM TCEP or CaM in 25 mM Tris-HCl buffer (pH 7.5) containing 50 mM NaCl that had been subjected to calcium ion removal as described above. Data were processed using the Origin software package with the iTC 200 plug-in. $CaCl_2$ solutions were prepared from 99.99% Ultradry grade (Sigma) and titrated into the ITC cell over 20 injections (1×0.4 μL followed by 19×2 μL) at a stock concentration of 275 μM for the WT VLDC, 250 μM for the EF-hand 1 mutein, 1.3 mM for the EF-hand 2 mutein, 300 μM for the EF-hand 3 mutein, and 2.4 mM for CaM. In a separate experiment, the WT VLDC was used at a concentration of 15 μM and $CaCl_2$ at 225 μM with the inclusion of 5 mM $MgCl_2$ in both solutions.

Inductively Coupled Plasma Optical Emission Spectroscopy. The concentration of calcium ions was determined using inductively coupled plasma optical emission spectroscopy

(ICP-OES) by the School of Environmental Sciences, University of East Anglia, Norwich, United Kingdom.

Stopped-Flow Spectrophotometry. Dissociation of calcium ions was detected by rapidly mixing calcium ion-loaded protein [1:1 (v/v)] with 2 mM Quin-2 and monitoring absorbance at 390 nm at 15 °C unless stated otherwise. The lower temperature was chosen to maximize the extent of calcium ion release observed. The high concentration of Quin-2 required for non-rate-limiting capture of calcium ions precluded fluorescence as a detection method because of excessive inner filtering effects. Furthermore, a wavelength of 390 nm was required with Quin-2 at such a high concentration to obtain an absorbance of ~1.0, which decreased in the presence of calcium ions. Data were collected using a Hi-Tech Scientific SF-61 DX2 stopped-flow spectrophotometer equipped with a 75 W Xe arc lamp (TgK Scientific, Bradford-on-Avon, United Kingdom). Unless otherwise stated, samples were formed in 10 mM Tris-HCl (pH 7.5) containing 50 mM NaCl and 1 mM TCEP. All protein solutions were adjusted to contain 100 μM $CaCl_2$ and 100 μM calcium ion binding sites before mixing (e.g., 33.3 μM VLDC with three sites and 14.4 μM AID-VLDC−CaM complex with seven sites) except for that of the VLDC EF-hand 1/2 mutein, which was 33.3 μM (33.3 μM protein with one site) because of its limited expression yield. Signals were calibrated by mixing 2 mM Quin-2 with either 20 mM EDTA, buffer only, 50 μM $CaCl_2$, or 100 μM $CaCl_2$. Control experiments confirmed that Quin-2 bound free calcium ions within the dead time of the equipment (~1 ms). Data were collected in at least triplicate and analyzed in the Hi-Tech Scientific KinetAssist3 software package.

Stopped-flow spectrofluorimetry was conducted as described above except that the instrument was in fluorescence mode and equipped with a 100 W Hg arc lamp. The excitation and emission wavelengths were 290 and >320 nm, respectively. Samples containing protein (5 μM each), 0.1 mM $CaCl_2$, and buffer [10 mM Tris-HCl (pH 7.5), 50 mM NaCl, and 1 mM TCEP] were mixed with 2 mM EDTA in buffer.

Surface Plasmon Resonance. Surface plasmon resonance (SPR) spectroscopy was conducted using a Biacore T100 instrument (GE Healthcare). A sample of the AID-VLDC in 10 mM ammonium acetate (pH 4) was immobilized onto a Biacore CM5 chip using amine coupling. The reference cell was prepared with ethanolamine as the blocking agent. Binding experiments were performed with 50 mM Tris-HCl buffer (pH 7.5) containing 150 mM NaCl, 0.1 mM $CaCl_2$, and 0.005% P20 surfactant. CaM was injected over the surface, and surfaces were regenerated with 2 mM EDTA. Data were analyzed using the Biacore T100 evaluation software (GE Healthcare).

RESULTS

Expression and Properties of CCaMK Constructs. Expression and purification of the full-length recombinant *M. truncatula* CCaMK were possible with or without a His tag or glutathione *S*-transferase fusion. However, size exclusion chromatography and dynamic light scattering showed that the full-length protein immediately started to form large aggregates that increased in mass with time (data not shown). EDTA and high NaCl concentrations promoted aggregation, and although the rate of aggregation was decreased slightly in the presence of dithiothreitol, glycerol, ADP, and $MgCl_2$, conditions were not found to prevent aggregation.

To study the binding of calcium ions to CCaMK and any associated conformational change, constructs were required to possess the EF-hands of CCaMK and not to aggregate. Two shorter constructs were therefore generated: one containing the autoinhibitory and visinin-like domains (AID-VLDC; CCaMK residues 318−523) and one containing the visinin-like domain alone (VLDC; residues 347−523). The AID-VLDC could be readily purified using CaM affinity chromatography, and the VLDC had an N-terminal His tag to allow nickel affinity chromatography. Both constructs were further purified using size exclusion chromatography to homogeneity (Figure S3 of the Supporting Information). The constructs existed as monomers in solution according to analytical ultracentrifugation (AUC) (Table 1) and remained stable over time as a single species according to size exclusion chromatography and dynamic light scattering (data not shown).

Table 1. AUC of Proteins and Their Complexes in the Presence of 2 mM Calcium Ions

protein (μM)	expected molecular mass[a] (kDa)	observed molecular mass (kDa)
VLDC (125)[b]	21.1	20.8 ± 0.1
AID-VLDC (50)	23.5	17.7 ± 0.2
CaM (50)	16.7	14.4 ± 0.01
AID-VLDC (50) with CaM (50)	40.2	34.9 ± 0.2

[a]Molecular mass expected per monomer or 1:1 complex. [b]Data were collected at 10000, 15000, and 20000 rpm with this sample and at 10000, 20000, and 30000 rpm for the remaining samples.

Experimental Evidence of the Existence of Three Functional EF-Hands in CCaMK. CCaMK has been reported to possess three EF-hands based on sequence alignments.[11] This was surprising because EF-hands normally exist in pairs.[17] Inspection of the sequence of *M. truncatula* CCaMK revealed the existence of the majority of the motif of a fourth EF-hand upstream of the three already identified (Table 2). A similar observation has recently been made with the *L. japonicas* CCaMK,[16] giving EF-hands 0−3 (Figure 1). The substitution of the Z ligand associated with the binding of a calcium ion to EF-hand 0 shows that it is the least well conserved of the four EF-hands, resulting in it being potentially missed by motif-seeking algorithms. Furthermore, an additional substitution of the normally highly conserved Gly at position 6 suggests that EF-hand 0 is functionally compromised, leaving only three sites capable of binding a calcium ion each as previously assumed. Both EF-hands 0 and 2 have substitutions of their −*Y* ligands (Table 1). However, because the protein backbone interacts with the calcium ion at position −*Y*, such side chain substitutions are normally tolerated.[17]

An electrospray ionization mass spectrometry (ESI-MS) approach was used to establish how many and which EF-hands are functional in CCaMK. All species in the mass spectrum of the VLDC in the presence of 100 μM EDTA were either the apoprotein or sodium adducts thereof (Figure 2A). In the presence of 100 μM calcium ions, the dominant species had three calcium ions bound (Figure 2B) and there was no evidence of a species with four calcium ions bound, even with 200 μM calcium ions (data not shown). These observations provide the first experimental evidence that CCaMK has three EF-hands that are capable of binding one calcium ion each.

To identify which EF hands are functional, EF-hands 1−3 were each mutated by substituting the first residue of their motifs from a normally invariant Asp to an Ala (Table 2), a

Table 2. EF-Hands of *M. truncatula* CCaMK at Loop Positions 1−12[a]

	1	2	3	4	5	6	7	8	9	10	11	12
ligand to Ca^{2+}	*X*		*Y*		*Z*		*−Y*		*−X*			*−Z*
most common[b]	D	K	D	G	D	G	T	I	D	F	E	E
frequency (%)[b]	100	29	76	56	52	96	23	68	32	23	29	92
also observed[b]		A	N	K	S		K	V	S	K	D	D
		T		R	N		X[c]	L	T	X[c]	K	
		R		N					E		X[c]	
		X[c]							X[c]			
EF-hand 0 (380)[d]	D	R	D	N	A	T	L	S	E	F	E	E
EF-hand 1 (413)[d]	D	N	N	R	D	G	T	V	D	M	R	E
EF-hand 2 (449)[d]	D	T	D	R	S	G	C	I	S	K	E	E
EF-hand 3 (491)[d]	D	A	N	N	D	G	K	V	T	F	D	E

[a]The EF-hand loop peptide sequences of CCaMK are shown in the context of the sequence motif observed in functional EF-hands.[17] Amino acid residues conforming to the motif are underlined. [b]Most commonly observed amino acid residues according to Gifford et al.[17] [c]Some other amino acid residues not present in the EF-hands of CCaMK are also frequently observed.[17] [d]Number of the first amino acid residue of the *M. truncatula* CCaMK protein sequence.

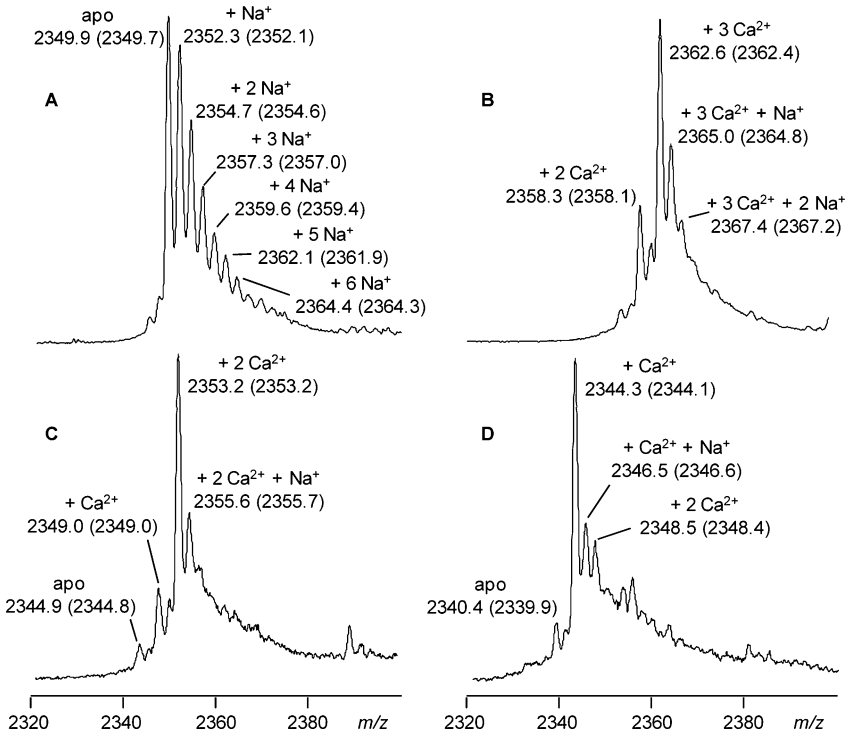

Figure 2. VLDC that is capable of binding three calcium ions according to ESI-MS. The spectra show the −9 charge series of ions associated with the VLDC and some if its muteins. While the −9 charge series was the most dominant in almost every case, all charge series (typically from −8 to −17) gave essentially identical distributions of species (data not shown). The assignment of peaks is indicated together with the observed (and predicted) values of *m*/*z*. (A) Spectrum of the VLDC (21156 kDa) in the presence of 100 μM EDTA, where the apoprotein was the dominant species. (B) Spectrum of the VLDC in the presence of 100 μM calcium acetate, where a species with three calcium ions bound was dominant and a species with four calcium ions bound (predicted *m*/*z* 2366.6) was not observed. (C) Equivalent spectrum of the VLDC EF-hand 1 mutein (21112 kDa), where a species with two calcium ions bound was dominant and a triply bound species (predicted *m*/*z* 2357.5) was not observed. (D) Equivalent spectrum of EF-hand 1/2 mutein (21068 kDa), where a singly bound species was dominant and only a trace of a doubly bound species was detected.

strategy used successfully in other systems.[27,28] Thus, a series of muteins were generated with either one or a combination of two EF-hands disabled (although EF-hand muteins 2 and 1/2 expressed less well than the wild type and mutein 2/3 did not seem to be expressed at all). ESI-MS of the VLDC EF-hand 1 mutein in the presence of calcium ions gave predominantly a species with two calcium ions bound and none with three (Figure 2C). The doubly bound species was also dominant with each of the EF-hand 2 and 3 muteins (data not shown). The EF-hand 1/2 mutein gave predominantly a singly bound species (Figure S2D of the Supporting Information) with only a trace of the doubly bound species. The singly bound species was also dominant in the EF-hand 1/3 mutein (data not shown). These results provide strong evidence that EF-hands 1−3 are each functional and that EF-hand 0 is not, providing direct experimental evidence of the bioinformatic predictions.

Binding of Calcium Ions to the EF-Hands of CCaMK Exposes Hydrophobic Surfaces. EF-hand proteins undergo conformational changes on binding calcium ions.[17] This is expected to be the case with CCaMK because calcium ions

dx.doi.org/10.1021/bi300826m | *Biochemistry* 2012, 51, 6895−6907

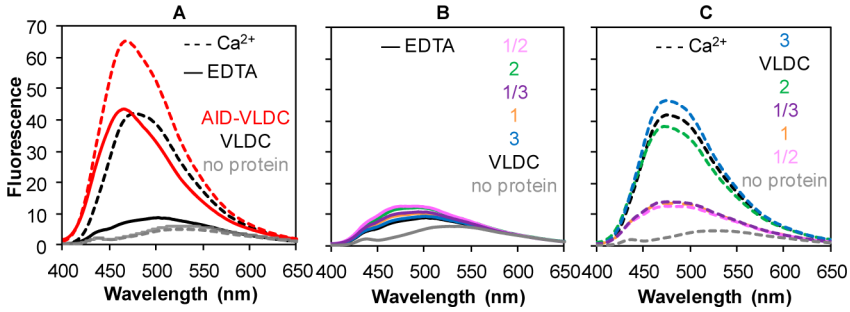

Figure 3. Calcium-dependent increase in ANS fluorescence with the AID-VLDC, VLDC, and VLDC EF-hand muteins. (A) Fluorescence spectra of ANS in the presence of either the AID-VLDC (red lines), the VLDC (black lines), or no protein (gray lines) with either 2 mM $CaCl_2$ (dashed lines) or 2 mM EDTA (solid lines). The increase in fluorescence demonstrated the exposure of hydrophobic protein surfaces in the presence of calcium. (B) Corresponding spectra of the VLDC and VLDC EF-hand muteins in the presence of EDTA (as annotated in color). (C) Equivalent spectra in the presence of calcium ions (as annotated in color). The disruption of EF-hand 1 reduced the calcium-dependent increase in fluorescence.

regulate this protein.[13] The only reported experimental evidence of this is a calcium ion-dependent shift in mobility of CCaMK using sodium dodecyl sulfate−polyacrylamide gel electrophoresis (SDS−PAGE).[13,16] Such evidence is potentially ambiguous because a change in mobility could be the result of a change in either the net charge or the susceptibility to SDS denaturation. In addition, calcium ions carry the opposite charge to proteins in the presence of SDS, leading to the potential loss of all but the most tightly bound ions from the proteins during electrophoresis.

A defining feature of EF-hand proteins, such as CaM, is the exposure of a hydrophobic cleft between the N- and C-terminal domains of two pairs of EF-hands allowing the binding of a target peptide.[17] The exposure of hydrophobic surfaces in EF-hand proteins can be conveniently monitored by an increase in the fluorescence of a reporter dye, ANS.[24] With the VLDC, ANS fluorescence was minimal in the presence of EDTA and increased markedly in the presence of calcium ions (Figure 3A) but not in the presence of magnesium ions (data not shown). A calcium-dependent increase was also seen with the AID-VLDC (Figure 3A). This provides unambiguous evidence that the EF-hands of CCaMK undergo a calcium-dependent conformational change analogous to those of other EF-hand proteins.

Interestingly, some background ANS fluorescence was also observed with the AID-VLDC in the presence of EDTA, implying hydrophobic patches on its additional AID peptide (318-PEIVSRLQSFNARRKLRAAAIASVWSSTI-346) may have given rise to this signal.

An analysis of the VLDC EF-hand muteins showed that they all behaved like the wild-type VLDC with the exception of muteins that included the disruption of EF-hand 1 (Figure 3B,C). In these cases, the fluorescence increase in the presence of calcium ions was diminished, implying the extent or character of the conformational change was somehow different when EF-hand 1 was not functional.

The Conformational Change Does Not Involve a Change in Net Secondary or Quaternary Structure. To establish whether the secondary structure of the AID-VLDC of CCaMK changes in a calcium ion-dependent manner, far-UV spectra were recorded and analyzed (Figure S4A and Table S1 of the Supporting Information). The data show that the protein was predominantly helical in the presence of 2 mM EDTA (64 ± 2%) with the remainder consisting of strand (5%), turns (11%), and unordered structure (19%). This distribution of secondary structure is typical of EF-hands.[17] In the presence of 2 mM calcium ions, the CD spectral peak maximum shifted by ∼0.5 nm, a phenomenon also observed with calbindin-D_{28K}.[29] In addition, the amount of helix increased by only 3% at the expense of unordered structures, while magnesium ions had an even weaker effect. Thus, any net change in secondary structure is very small, consistent with many other EF-hand proteins.[17]

The VLDC had less helical content in the presence of EDTA [60 ± 2% (Table S1 of the Supporting Information)] than the AID-VLDC. While the VLDC was 178 amino acids long (including its extra N-terminal Met residue) giving 107 ± 4 residues in helical conformations, the AID-VLDC was 213 amino acids long (including its extra N-terminal Met residue and His_6 tag) giving 136 ± 4 residues in helical conformations. Thus, there were 29 ± 6 more residues in a helical conformation in the AID-VLDC than in the VLDC. It is therefore highly likely that the extra 29 amino acids of the AID-VLDC that are associated with the AID are α-helical. This is consistent with other CaM-binding peptides that are α-helical such as that in CaMKII.[30]

The helical content of the VLDC changed by ≤1% in the presence of either calcium or magnesium ions despite an ∼1 nm shift in the spectral maximum in the presence of calcium ions (Figure S4A of the Supporting Information). Therefore, as with the AID-VLDC, the net secondary structure of the VLDC did not change significantly in the presence of calcium ions. It therefore seems likely that the AID in the AID-VLDC remains helical regardless of the presence of calcium ions.

The VLDC EF-hand 1, 3, and 1/3 muteins had helical contents similar to that of the VLDC (Table S1 and Figure S4B of the Supporting Information), suggesting their secondary structures were not significantly perturbed by their amino acid substitutions. EF-hand 2 and 1/2 muteins had ∼10% less helical content, suggesting some perturbation of secondary structure associated with disruption of EF-hand 2. Interestingly, the shift in the spectral peak maximum was not observed in any mutein with EF-hand 1 disrupted, suggesting the shift is associated with occupancy of this EF-hand.

The presence of not only EF-hands that expose a hydrophobic surface in a calcium-dependent manner but also a CaM-binding peptide in the AID-VLDC opens up the possibility that these parts of the protein could interact with each other intermolecularly. However, AUC (Table 1), size exclusion chromatography, and dynamic light scattering (data not shown) showed that this protein construct existed as a monomer regardless of the the presence of calcium ions, precluding such an intermolecular interaction. Therefore, these

dx.doi.org/10.1021/bi300826m | *Biochemistry* 2012, 51, 6895−6907

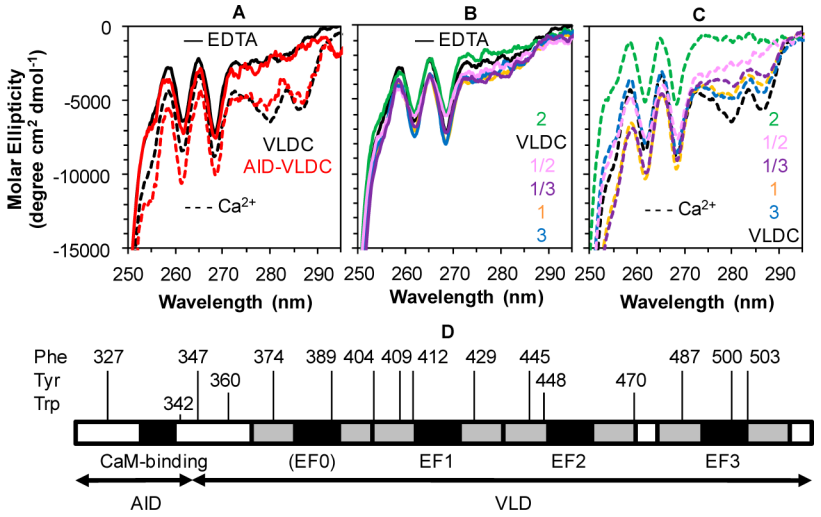

Figure 4. Near-UV CD spectra of the AID-VLDC, VLDC, and VLDC EF-hand muteins in the presence of either EDTA or calcium ions. (A) Near-UV CD spectra of the VLDC (black lines) and the AID-VLDC (red lines) in the presence of either 2 mM EDTA (solid lines) or 2 mM $CaCl_2$ (dashed lines). (B and C) Equivalent spectra of the VLDC EF-hand 1, 2, 3, 1/2, and 1/3 muteins (as annotated in color) in the presence of EDTA and $CaCl_2$, respectively. The spectra for the VLDC (black line) from panel A are plotted again in panels B and C to aid comparisons. (D) Occurrence of Phe, Tyr, and Trp residues within the AID-VLDC. Amino acid sequence numbers refer to full-length *M. truncatula* CCaMK.

observations showed that there was no change in quaternary structure on binding calcium ions.

The Conformational Change Involves a Change in Tertiary Structure. Near-UV CD spectroscopy provides information about the relative environments of aromatic amino acid side chains.[31] The side chains of Phe, Tyr, and Trp can give signals in the ranges of 250−270, 250−295, and 250−305 nm, respectively. The more solvent-exposed the side chain, the less chiral the environment it will experience leading to a smaller CD signal.

The near-UV CD spectra of the VLDC and AID-VLDC showed significant negative signals likely to arise from both Phe and Tyr residues (Figure 4). A lack of significant difference between the spectra of the two constructs suggested the Trp342 residue that is present in only the AID-VLDC gave no significant signal, likely because it is solvent-exposed. Perhaps this residue contributed to the background ANS fluorescence with the AID-VLDC described above.

The spectra of both constructs changed in a calcium-dependent manner, showing that the environments of the Phe and Tyr residues changed as a result of a conformational change. The spectra associated with the AID-VLDC changed slightly more in the 250−270 region, implying the additional Phe residue of the AID also experienced a change in its environment.

The spectra of the VLDC EF-hand muteins in the presence of EDTA were very similar to that of the wild-type protein (Figure 4B), suggesting they all had very similar structures. By contrast, there were significant differences in the spectra in the presence of calcium ions (Figure 4C), suggesting that the ability of the muteins to undergo the calcium ion-dependent conformational change was altered in some cases. A difference common to all muteins in the presence of calcium ions was a weaker signal (less negative) in the 270−295 nm region, which would be associated with one or more of three Tyr residues [Tyr360 near the N-terminus of these constructs and Tyr448 and Tyr470 flanking EF-hand 2 (Figure 4D)]. A loss of signal across the whole 250−295 nm region was observed with EF-hand 2 mutein, particularly above 270 nm indicating no signal from Tyr residues. Therefore, occupancy of EF-hand 2 by a calcium ion is important for the conformational change. It is also possible, but not certain, that the Tyr residues that flank EF-hand 2 are responsible for most of the Tyr signal in the wild-type VLDC in the presence of calcium ions.

Both the VLDC EF-hand 1 and 1/3 muteins exhibited an increased signal magnitude in the 250−270 nm region in the presence of calcium ions, compared with that of the wild-type protein. The occupancy of EF-hand 1 is therefore also important in the conformational change. This may also suggest the disruption of EF-hand 1 leads to a relative change in the environment of the Phe residues within this EF-hand. The spectrum of EF-hand 1/2 mutein in the 250−270 nm region appeared to display a compromise between the increase and decrease in the magnitude of the signal associated with the disruption of EF-hands 1 and 2, respectively, consistent with the two effects being additive.

EF-hand 3 mutein had a wild-type-like spectrum in the 250−270 nm region. Consistent with this was the similarity in this region of the spectra associated with EF-hand 1 and 1/3 muteins. Either occupancy of EF-hand 3 is not required for the conformational change, or there are no amino acid side chains that report on its occupancy. It is also possible that the Phe residues of EF-hand 3 do not contribute to the signals.

Affinity for Calcium Ions. The affinity of the VLDC for calcium ions was determined using ITC. The binding curve (Figure 5) could be fit to a model with 1.79 ± 0.02 identical noninteracting independent sites with a K_d of 200 ± 50 nM and favorable changes to both enthalpy and entropy (Table 3). Because of the quality of the fit to this simple model, there was no compelling evidence of cooperativity and we could not distinguish the affinities of the two sites observed. As three binding sites for calcium ions per subunit were expected, the protein sample was subjected to inductively coupled plasma optical emission spectroscopy (ICP-OES) to establish the calcium ion contamination level that remained despite attempts to minimize it using solid phase chelators. The level of contamination of the protein sample was 1 order of magnitude higher than that of buffer alone. If all of the contaminating

dx.doi.org/10.1021/bi300826m | *Biochemistry* 2012, 51, 6895−6907

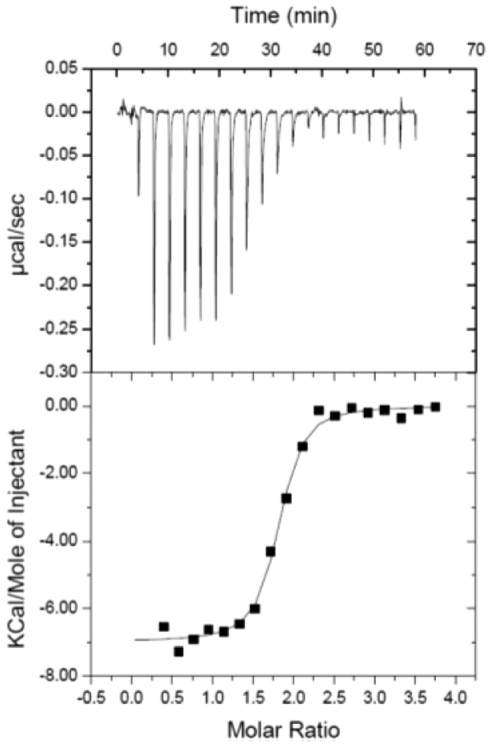

Figure 5. ITC of the binding of calcium ions to the VLDC. The isotherm associated with the titration of calcium ions into a VLDC (15 μM) sample at 25 °C is shown (top). The bottom panel shows the integrated data together with a best fit line using a model with one type of noninteracting independent binding site giving a K_d of 200 ± 50 nM and 1.79 sites (see Table 3).

calcium ions were bound to the protein, only 2.1 sites per subunit would have remained unoccupied (Table 3), which was reasonably consistent with the number of sites observed using ITC. One can therefore conclude that there was likely to be one site that had a significantly higher affinity for calcium ions (≤20 nM) than the two that were observed by ITC.

When the experiment was repeated in the presence of 5 mM magnesium ions, the K_d increased only modestly to 300 ± 30 nM, showing that magnesium ions have a very low affinity for the VLDC and compete poorly with calcium ions. Because the cytoplasmic concentration of magnesium ions in plant cells approximates to 0.4 mM,[32] it would appear unlikely that these ions would affect the affinity for calcium ions significantly in planta.

To establish which site is the high-affinity site, the VLDC EF-hand 1−3 muteins were also assessed using ITC (Table 3 and Figure S5 of the Supporting Information). The mutein that gave the largest number of observed sites was that with EF-hand 3 disrupted. A total of 1.66 ± 0.3 sites were observed with 2 theoretical sites remaining and 1.6 expected when calcium ion contamination was taken into account. The number of sites observed with the other two muteins was close to 1. It therefore follows that EF-hand 3 is the high-affinity site.

Disruption of EF-hand 3 led to a modest 3.5-fold increase in the observed K_d (Table 3), presumably because of some weak influence on the ability of EF-hands 1 and 2 to function normally. Disruption of EF-hand 1 had the smallest effect on K_d, which increased by 1.6-fold. Interestingly, the entropic contribution to binding became slightly unfavorable, implying some change in the behavior of this mutein. The largest effect on K_d was observed with EF-hand 2 disrupted, giving an ∼30-fold increase that was reflected mostly in a loss of a favorable entropic contribution to binding. The largest discrepancy between the number of sites per subunit observed by ITC and ICP-OES was with this mutein, implying that this construct might not have been functionally homogeneous.

Dissociation of Calcium Ions. The interpretation of calcium spiking by CCaMK is expected to be governed by the kinetics of the system and not just the affinities between each species involved because spiking is a nonequilibrium phenomenon. The rate at which the protein constructs release calcium ions was therefore determined by rapidly mixing calcium ion-loaded proteins with Quin-2, a calcium ion-responsive dye, using stopped-flow spectrophotometry.[24]

A calcium ion dissociation rate constant for the VLDC was determined to be 2.11 ± 0.01 s^{-1} (Table 4 and Figure S6 of the Supporting Information). By comparison with controls, it was clear that 1.5 of the 3 theoretical calcium ions per subunit were observed to dissociate. Attempts to fit the observed data to two-exponential functions failed to satisfactorily resolve the properties of 1.5 observable sites. Experimental conditions were such that it was expected that >99% of the binding sites were preloaded with calcium ions based on the measured affinities (Table 3). It was therefore apparent that the remaining 1.5 calcium ions must have dissociated before we could begin the measurement (dead time of ∼1 ms) and therefore with a rate constant of >500 s^{-1}. Although it was not

Table 3. ITC and ICP-OES Data for Calcium Ions Binding to either the VLDCs or CaM

protein	no. of sites expected[a]	sites observed by ICP-OES[b]	sites observed by ITC[c,d]	K_d[d] (nM)	ΔH^d (kJ mol^{-1})	ΔS^d (J mol^{-1} K^{-1})	$\Delta G^{\circ d}$ (kJ mol^{-1})
VLDC	3	2.1	1.79 ± 0.02	200 ± 50	−33.1 ± 0.6	24	−40
VLDC EF-hand 1 mutein	2	1.2	1.07 ± 0.01	325 ± 60	−37.7 ± 0.7	−2	−37
VLDC EF-hand 2 mutein[e]	2	1.5	0.80 ± 0.01	5800 ± 600	−22.2 ± 0.6	25	−30
VLDC EF-hand 3 mutein	2	1.6	1.66 ± 0.03	700 ± 100	−29.6 ± 0.7	19	−35
CaM	4	3.3	1.1 ± 0.1	1000 ± 500	−0.6 ± 0.6	113	−34
			1.8 ± 0.2	15000 ± 3000	−13 ± 2	48	−28

[a]Number of calcium ion binding sites per protein subunit expected. [b]The number of free calcium-binding sites per protein subunit was estimated by subtracting the calcium ion concentration of protein samples determined using ICP-OES from the total expected concentration of sites followed by dividing the resultant value by the protein subunit concentration. [c]Number of calcium ion binding sites per protein subunit observed according to ITC. [d]ITC data for the VLDCs and CaM were fit with a model involving identical independent noninteracting sites and two types of independent noninteracting sites, respectively. [e]Concentration of 75 μM for this mutein, 15 μM for the other VLDCs, and 60 μM for CaM.

dx.doi.org/10.1021/bi300826m | *Biochemistry* 2012, 51, 6895−6907

Table 4. Dissociation of Calcium Ions

protein(s)	no. of sites expected[a]	no. of sites observed[b]	k_{off}[c] (s^{-1}) fast	medium	slow
VLDC	3	1.5	nd[d]	2.11 ± 0.01	nd[d]
AID-VLDC	3	2.0	4.0 ± 0.2	0.57 ± 0.01	nd[d]
CaM	4	2.5	19.6 ± 0.2	0.615 ± 0.004	nd[d]
AID-VLDC with CaM	7	5.5	4.96 ± 0.06	0.54 ± 0.01	0.123 ± 0.002
	na[e]	na[e]	4.61 ± 0.06[f]	0.53 ± 0.01[f]	nd[d]
VLDC EF-hand 1 mutein	2	1.0	12.8 ± 0.2	1.55 ± 0.02	nd[d]
VLDC EF-hand 2 mutein	2	1.0	15.2 ± 0.3	2.55 ± 0.06	nd[d]
VLDC EF-hand 3 mutein	2	1.0	nd[d]	5.03 ± 0.03	nd[d]
VLDC EF-hand 1/2 mutein	1	1.0	nd[d]	nd[d]	nd[d]
VLDC EF-hand 1/3 mutein	1	0	nd[d]	nd[d]	nd[d]

[a]Number of calcium ions per subunit expected. [b]Number of calcium ions per subunit observed to dissociate. [c]First-order dissociation rate constants of calcium ions were determined using stopped-flow spectrophotometry by mixing calcium ion-loaded proteins with Quin-2 and monitoring absorbance at 390 nm. Time courses fit best to either one-, two-, or three-exponential functions. [d]Not determined. [e]Not applicable. [f]These rate constants were determined using stopped-flow fluorescence spectroscopy of the Trp of the AID-VLDC (Figure 4D) using excitation and emission wavelengths of 290 and >320 nm, respectively.

possible to resolve the individual dissociation rate constants for each of the three EF-hands, it was possible to establish that there are at least two types that differ by at least 2 orders of magnitude. Similar results have been reported for other EF-hand proteins, including CaM, where its N-terminal lobe releases calcium ions with a rate constant of >850 s^{-1}.[33]

Two of the three expected calcium ions were observed to dissociate from the AID-VLDC. In this case, it was possible to resolve two exponential phases with amplitudes on the same order of magnitude giving rate constants of 4.0 ± 0.2 and 0.57 ± 0.01 s^{-1} (Table 4, Figure 6, and Figure S6 of the Supporting Information). There must again have been a very rapid rate constant (>500 s^{-1}) associated with the release from a site that was not observable. The presence of the AID in this construct therefore had a small influence on the dissociation rate constants such that three could now be resolved.

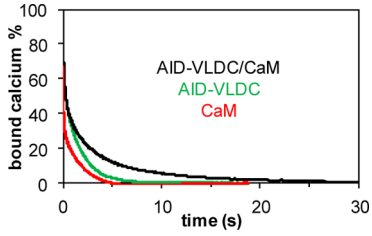

Figure 6. Dissociation of calcium ions from CaM, the AID-VLDC, and the AID-VLDC−CaM complex. The dissociation of calcium ions from protein was monitored using stopped-flow spectrophotometry with Quin-2. The data are plotted as a percentage of total calcium binding site concentrations expected. The most rapid dissociation was that from CaM (red line; k_{off} = 0.615 ± 0.004 and 19.6 ± 0.2 s^{-1}), with the AID-VLDC (green line; also shown in Figure S6 of the Supporting Information; k_{off} = 0.57 ± 0.01 and 4.0 ± 0.2 s^{-1}) and the AID-VLDC−CaM complex (black line; k_{off} = 0.123 ± 0.002, 0.536 ± 0.009, and 4.96 ± 0.06 s^{-1}) giving progressively slower dissociation (see Table 4).

It was reasonable to predict that the very fast rate constant was associated with EF-hands 1 and/or 2 to reflect the relatively low affinities of these sites (Table 3). The experiment was therefore repeated with the VLDC EF-hand muteins (Table 4) to resolve the identities of the very fast and slower dissociating EF-hands. One of two ion release events was detected with EF-hand 1 mutein, implying this EF-hand was not the one with the very fast release kinetics. Surprisingly, two exponential functions that differed by 1 order of magnitude were required to fit the data despite only one net site being observed. This implies that other processes were partially rate-limiting and these could include the protein conformational change. Unexpectedly, similar observations were made with EF-hand 2 mutein, implying this site was not the very fast site either. It must be noted that even though the affinity of this mutein for calcium ions is the poorest of those tested (Table 3), its sites would have been expected to be >90% preloaded in the stopped-flow experiment. EF-hand 3 mutein also gave a similar result, except that only one intermediate rate constant could be resolved. Therefore, the very fast release site could not be identified by disrupting single EF-hands.

The one potential calcium ion was observed to be released from EF-hand 1/2 mutein, implying that EF-hands 1 and 2 together participate in the very fast release event. The kinetics of the observable process could not be satisfactorily fit even with three exponential functions, suggesting other processes being somewhat rate-limiting also with this construct. Zero of one calcium ion release was observed with EF-hand 1/3 mutein, suggesting that EF-hand 2 can release calcium ions very quickly. In conclusion, EF-hands 1 and 2 probably contribute to the very fast release event, and EF-hand 3 likely dominates the observable calcium ion release event. In addition, the kinetics of the release of calcium ions is complex and could involve a partially rate-limiting conformational change.

Although it has not been possible to assign specific equilibrium and dissociation rate constants to each EF-hand, it was possible to calculate the likely magnitudes of the association rate constants. The affinity of EF-hands 1 and 2 for calcium ions was 200 nM (Table 3), so if the k_{off} was 500 s^{-1}, it follows that k_{on} would be ~10^9 M^{-1} s^{-1}. Similarly, the affinity of EF-hand 3 for calcium ions was the highest (say 20 nM), and its associated k_{off} appeared to be 2.11 s^{-1} (Table 4), giving a k_{on} of ~10^8 M^{-1} s^{-1}. Although these are merely estimates of k_{on} values (noting that they are also based on data sets obtained at different temperatures of 15 and 25 °C), they appear to indicate that the association of calcium ions to each of the EF-hands is rapid and probably limited by diffusion rate.

Properties of *M. truncatula* CaM. AUC showed that *M. truncatula* CaM exists as a monomer in solution (Table 1),

dx.doi.org/10.1021/bi300826m | *Biochemistry* 2012, 51, 6895−6907

which is typical for a canonical CaM.[17] ITC showed that CaM exhibited two types of calcium ion-binding site that had affinities of 1 ± 0.5 and 15 ± 3 μM, the former having a greater entropic component (Table 3). The presence of two types of sites was clear from the presence of distinct phases in the titration (Figure S5D of the Supporting Information). These observations are consistent with *Drosophila* CaM having distinguishable affinities of 2 and 13 μM associated with its N and C-terminal domains, respectively, where the former comprises the lower-affinity EF-hand pair.[33]

Two values of k_{off} (19.6 ± 0.2 and 0.615 ± 0.004 s^{-1}) with similar amplitudes were distinguishable for the release of calcium ions from CaM using stopped-flow spectrophotometry (Table 4 and Figure 6). A total of 2.5 of 4 sites were observed to dissociate, showing that 1.5 sites released their calcium ions with a rate constant of >500 s^{-1} (noting that CaM would be expected to have been >90% loaded at the start of the experiment). By comparison with *Drosophila* CaM (with k_{off} values of 11.8 and >850 s^{-1}), it would appear that the very fast rate is probably associated with the N-terminal domain.[33] It is therefore likely that the limiting k_{on} values for the N- and C-terminal domains of *M. truncatula* CaM are 3×10^7 and 6×10^5 M^{-1} s^{-1}, respectively, both close to or at diffusion rate limitation.

Interaction between the AID-VLDC and CaM. CCaMK is known to bind to CaMs in a calcium ion-dependent manner,[14] and sequence analysis has suggested the presence of one binding site for CaM in the AID.[13] AUC clearly showed that a 1:1 complex was indeed formed between CaM and the AID-VLDC (Table 1).

The observed dissociation of calcium ions from the complex was slower than from either of the individual proteins alone (Figure 6), as would be expected for a stable tripartite complex. Three values of k_{off} could be resolved with the complex (Table 4). Two (4.96 ± 0.06 and 0.54 ± 0.01 s^{-1}) were similar to those observed with the AID-VLDC alone, the slower of which was also similar to one observed with CaM. However, the third rate constant (0.123 ± 0.002 s^{-1}) was slower than all others measured, making the overall release of calcium ions from the complex the slowest.

CaM does not contain any tryptophan residues, but the AID-VLDC contains one within its AID (Figure 4). This provided the opportunity to monitor complex formation using fluorescence. When CaM bound to the AID-VLDC in a calcium ion-dependent manner, there was a shift in the tryptophan fluorescence emission spectrum (Figure S7 of the Supporting Information). This made it possible to monitor the EDTA-induced dissociation of the complex using stopped-flow spectrofluorimetry (Figure S8 of the Supporting Information). Two rate constants could be resolved from the time course [4.61 ± 0.06 and 0.53 ± 0.01 s^{-1} (Table 4)] that were very similar to the two faster rate constants determined for the dissociation of calcium ions [4.96 ± 0.06 and 0.54 ± 0.01 s^{-1}, respectively (Table 4)]. This implied the concerted release of some of the calcium ions with the dissociation of the proteins.

It was also possible to monitor the formation of the complex using SPR spectroscopy. The extent of complex formation exhibited a CaM concentration dependence as expected (Figure S9 of the Supporting Information). However, the kinetics were complex, precluding the ability to confidently fit the data to reasonable models. Nevertheless, plotting the extent of complex formation versus CaM concentration provided an estimate of the affinity between the two proteins of 46 ± 8 nM, which is similar to that determined between potato CaM and lily CCaMK of 55 nM.[14] In addition, the association rate constant appeared to be in the 10^4–10^6 M^{-1} s^{-1} range in the presence of calcium ions, but this was model-dependent. Most striking was the contrast between the very slow dissociation of the protein complex in the presence of calcium and the much faster dissociation in the presence of EDTA (i.e., absence of calcium ions), with rate constants estimated to be ~10^{-4} and ~0.1 s^{-1}, respectively.

DISCUSSION

The VLD of CCaMK Undergoes a Calcium Ion-Dependent Conformational Change. To study the calcium ion-dependent conformational change in CCaMK, two non-aggregating constructs were generated that each possessed the VLD. In general, the VLDC and the AID-VLDC behaved similarly, indicating that the presence of the AID had little effect on the properties of the VLD. While it is likely that the same is true in the presence of the kinase domain, the key findings presently described should be checked with a nonaggregating full-length construct of CCaMK when available.

Sequence analysis predicts the presence of three functional EF-hands in CCaMK,[11,16] and deletion or disruption of these EF-hands affects the properties of CCaMK in vitro and in vivo.[10,13,14,16] However, mass spectrometry has provided the first direct experimental evidence that EF-hands 1–3 are indeed each capable of binding a calcium ion (Figure 2) and that EF-hand 0 is not. The presence of an inactive EF-hand is not unusual because they have been observed in other proteins.[34,35] Occupancy of the functional EF-hands of CCaMK is known to promote autophosphorylation,[13] implying a calcium-dependent conformational change. A range of biophysical methods has provided unequivocal experimental evidence of such a conformational change. This change occurred at the tertiary level according to near-UV CD spectroscopy (Figure 4), with little change at the secondary level and no change at the quaternary level (Table 1 and Figure S4 and Table S1 of the Supporting Information).

The VLD was shown to be predominantly an α-helical protein (Figure S4 and Table S1 of the Supporting Information), while the AID appeared to be entirely α-helical as expected for a target of CaM such as the CaM-binding domain of CaMKII.[30] Near-UV spectroscopy suggested that the AID experiences a calcium-dependent change in its environment (Figure 4), but whether occupancy of the EF-hands of the VLD is required for the AID to be available for the binding of CaM remains to be elucidated.

The calcium-dependent exposure of a hydrophobic surface within the VLD is consistent with other EF-hand proteins.[17] This begs the question of why this occurs because in other EF-hand proteins it normally allows the binding of target peptides. Perhaps the VLD is capable of binding the AID. However, we have shown that no intermolecular interaction occurs between AID-VLDC constructs regardless of the presence of calcium ions. An intramolecular interaction appears unlikely in the presence of calcium ions because ANS is not excluded from binding to the hydrophobic surface with the AID present and the AID is the target of CaM under these conditions. An intramolecular interaction in the absence of calcium ions is similarly unlikely because the integrity of the VLD appeared to be similar regardless of the presence of the AID. In addition, the AID-VLDC gave a significant signal with ANS, implying the somewhat hydrophobic AID was accessible without calcium

ions present. These results are consistent with a report that the lily VLD does not bind its AID.[12] Therefore, the hydrophobic surface could interact with the kinase domain. Indeed, a conformational change in calcium-dependent protein kinases has been shown to involve the rearrangement of intramolecular hydrophobic interactions.[36] However, preliminary experiments suggest that the exposure of new hydrophobic surfaces still occurs with a full-length CCaMK protein construct that includes the kinase domain (J. Harrison and S. Bornemann, unpublished observations). It therefore remains possible that the VLD could bind to a phosphorylation target protein of CCaMK.

Contribution of Each EF-Hand. EF-hand 1 appears to be one of the lower-affinity calcium ion-binding sites with a K_d of 200 nM (Table 3) and could contribute to the very fast calcium ion release event with a rate constant of >500 s^{-1}. The disruption of this site led to less exposure of a hydrophobic surface in the presence of calcium ions (Figure 3), the loss of a small shift in the near-UV spectral maximum (Figure S4 of the Supporting Information), and some changes in the near-UV spectrum of the VLDC in the presence of calcium ions (Figure 4). Nevertheless, the modest change in the affinity for calcium ions of the EF-hand 1 mutein suggests that disruption of this site led to relatively modest disruption to the functionality of the VLD as a whole.

Like EF-hand 1, EF-hand 2 also appeared to have an affinity for calcium ions of 200 nM and was associated with the very rapid release of calcium ions. However, disruption of EF-hand 2, in contrast to EF-hands 2 and 3, appeared to affect the VLD severely. The VLDC EF-hand 2 mutein expressed less well: it had an altered secondary structure in the presence and absence of calcium ions (Figure S4 and Table S1 of the Supporting Information), its near-UV spectrum in the presence of calcium ions was significantly altered (Figure 4), and ITC analysis showed a significant impairment of the binding of calcium ions. These findings together imply the functional heterogeneity of this mutein (Table 3 and Figure S5 of the Supporting Information). Therefore, the integrity of EF-hand 2 appeared to be particularly important for the overall function of the VLD.

EF-hand 3 had the highest affinity for calcium ions (≤20 nM) and is presumably linked to the slowest calcium ion release rate. Like with EF-hand 1, disruption of EF-hand 3 led to an only modest change in the affinity for calcium ions (Table 3 and Figure S5 of the Supporting Information). It is noteworthy that a shift in the mobility of a *L. japonicus* VLDC via SDS−PAGE was abolished by disruption of EF-hand 3, but not 1 or 2,[16] and, in the case of the equivalent lily protein, by disruption of EF-hand 3 and to a small extent EF-hand 2.[13] This might have reflected the high affinity of EF-hand 3 for calcium ions rather than the dominance of this EF-hand in a conformational change given the limitations of SDS−PAGE (see above). Interestingly, it is the disruption of EF-hand 3 in *L. japonicus* CCaMK that led to the most severe compromise in the accommodation of rhizobia and mycorrhizae.[16]

Each EF-hand clearly contributed differently to the calcium ion-dependent conformational change and functionality of the VLD. The complexity of this functionality was reflected in the kinetics of the release of calcium ions from the VLD. Although the kinetics of the binding of calcium ions has not been determined directly, estimates of the rate constants suggest that binding is very likely to be at or near the diffusion rate limitation.

Overall, it would appear that all three EF-hands are important for the full functionality of the VLD. That each EF-hand is important is consistent with reports of the effect of disrupted or deleted EF-hands of CCaMK on autophosphorylation, target phosphorylation, the accommodation of rhizobia, and mycorrhization.[12,14,16]

Implications for the Interpretation of Calcium Spiking. The basal intracellular calcium ion concentration within a *Medicago sativa* root hair cell is 125−150 nM,[37] while the peak concentration during calcium spiking is 500−700 nM higher, giving 625−850 nM.[3] This range appears to be reasonably well matched to the K_d value of 200 nM associated with EF-hands 1 and 2. Because the affinity of EF-hand 3 is much greater, it is likely to be occupied at basal calcium ion concentrations. Therefore, while all three EF-hands have important structural roles, only EF-hands 1 and 2 appear to be poised to respond to calcium spiking.

We have also studied the calcium ion binding properties of *M. truncatula* CaM 1. Although its K_d values of 1 and 15 μM are typical for canonical CaMs,[33] they are 1 or 2 orders of magnitude higher than the calcium ion concentration at the peak of a spike. However, the affinity of CaMs for calcium ions can increase 1 or 2 orders of magnitude in the presence of a target peptide, potentially compensating for this apparent discrepancy.[33] Consistent with this is the observation that the ability of lily CCaMK to bind CaM is compromised when the calcium ion concentration is in the 100 nM range.[14]

The association of calcium ions to both the VLD and CaM was estimated to be at or near the diffusion rate limitation. It therefore follows that when the calcium ion concentration increases in the ∼10 s up phase of a spike, a new equilibrium position where both proteins have more calcium ions bound will be substantially reached within this time frame. The formation of a CCaMK−CaM complex would subsequently occur because the binding of CaM to CCaMK is calcium ion-dependent. This is reflected in the calcium ion-dependent decrease in the K_d of CCaMK for CaM by several orders of magnitude to 55 nM[14] with a corresponding decrease in k_{off} from ∼0.1 to ∼10^{-4} s^{-1} according to SPR spectroscopy (Figure S9 of the Supporting Information). The down phase of a spike then occurs on a slightly longer time scale but is nevertheless complete well before the next spike, which typically has a periodicity of 90 s.[3] As the calcium ions are removed from the system by pumps in the membranes of the calcium ion stores, the ions will dissociate from both the VLD and CaM, regardless of whether they are in a protein complex with each other, with k_{off} rate constants of at least 0.123 ± 0.002 s^{-1} (Table 4 and Figure 6), i.e., with half-lives of ≤5.6 s. Preliminary experiments with a full-length CCaMK construct suggest that the rate of release of calcium ion from the VLD is not influenced by the presence of the kinase domain (L. Zhou and S. Bornemann, unpublished observations). It therefore follows that CCaMK and CaM will lose their calcium ions essentially concomitantly with the down phase of a spike. According to both stopped-flow spectrofluorimetry (Table 4 and Figure S8 of the Supporting Information) and SPR spectroscopy (Figure S9 of the Supporting Information), CaM dissociates from the AID-VLDC on the same time scale as calcium ions dissociate from the protein complex when calcium ions are removed from the system. One can therefore conclude that the formation and dissociation of the CCaMK−CaM complex would substantially mirror calcium spiking.

dx.doi.org/10.1021/bi300826m | *Biochemistry* 2012, 51, 6895−6907

It is known that autophosphorylated CCaMK has an 8-fold higher affinity for CaM in the presence of calcium ions, giving a K_d of 6.5 nM,[14] suggesting that a protein complex between these two species would reach a higher level during each spike than in the absence of autophosphorylation. Unless the affinity of autophosphorylated CCaMK for CaM increases significantly in the absence of calcium ions and is due to a corresponding reduction in k_{off}, which seems unlikely,[14] the complex between autophosphorylated CCaMK and CaM would also substantially mirror calcium oscillations. The kinetics of autophosphorylation, cognate target protein phosphorylation, and dephosphorylation will require study in the future, not least because (auto)phosphorylation could persist between spikes allowing the integration and interpretation of calcium spiking with the opportunity for frequency or amplitude modulation as seen in animal systems.[38]

■ ASSOCIATED CONTENT

Supporting Information

Figures S1−S9 and Table S1. This material is available free of charge via the Internet at http://pubs.acs.org.

■ AUTHOR INFORMATION

Corresponding Author

*Department of Biological Chemistry, John Innes Centre, Norwich Research Park, Norwich NR4 7UH, United Kingdom. Phone: +44 (0)1603 450741. Fax: +44 (0)1603 450018. E-mail: stephen.bornemann@jic.ac.uk.

Funding

This work was supported by the United Kingdom Biotechnology and Biological Sciences Research Council through a Doctoral Training Grant and an Institute Strategic Programme Grant (BB/J004553/1), by the John Innes Foundation, and by the European Research Council through a "Symbiosis" Starting Grant to G.E.D.O.

Notes

The authors declare no competing financial interest.

■ ACKNOWLEDGMENTS

We thank Dr. Fiona Husband and Dr. Phil Johnson for assistance with CD experiments, Dr. Mike Naldrett and Dr. Gerhard Saalbach for help with mass spectrometry, Dr. Tom Clarke for assistance with analytical ultracentrifugation experiments, and Ben Miller, Dr. Akira Miyahara, Dr. Richard Morris, and Professor Dale Sanders for helpful discussions.

■ ABBREVIATIONS

CCaMK, calcium/calmodulin-dependent protein kinase; VLD, visinin-like domain; VLDC, visinin-like domain construct; AID, autoinhibitory domain; AID-VLDC, autoinhibitory domain with visinin-like domain construct; MS, mass spectrometry; CD, circular dichroism; ITC, isothermal calorimetry; ICP-OES, inductively coupled plasma optical emission spectroscopy; AUC, analytical ultracentrifugation; HEPES, 4-(2-hydroxyethyl)-1-piperazineethanesulfonic acid; TCEP, tris(2-carboxyethyl)phosphine; ESI-MS, electrospray ionization mass spectrometry; EGTA, ethylene glycol tetraacetic acid; ANS, 8-anilino-1-naphthalenesulfonic acid; EDTA, ethylenediaminetetraacetic acid; SPR, surface plasmon resonance.

■ REFERENCES

(1) Bonfante, P., and Requena, N. (2011) Dating in the dark: How roots respond to fungal signals to establish arbuscular mycorrhizal symbiosis. *Curr. Opin. Plant Biol. 14*, 451−457.

(2) Oldroyd, G. E. D., Murray, J. D., Poole, P. S., and Downie, J. A. (2011) The rules of engagement in the legume-rhizobial symbiosis. *Annu. Rev. Genet. 45*, 119−144.

(3) Ehrhardt, D. W., Wais, R., and Long, S. R. (1996) Calcium spiking in plant root hairs responding to *Rhizobium* nodulation signals. *Cell 85*, 673−681.

(4) Chabaud, M., Genre, A., Sieberer, B. J., Faccio, A., Fournier, J., Novero, M., Barker, D. G., and Bonfante, P. (2011) Arbuscular mycorrhizal hyphopodia and germinated spore exudates trigger Ca^{2+} spiking in the legume and nonlegume root epidermis. *New Phytol. 189*, 347−355.

(5) Miwa, H., Sun, J., Oldroyd, G. E. D., and Downie, J. A. (2006) Analysis of nod-factor-induced calcium signaling in root hairs of symbiotically defective mutants of *Lotus japonicus*. *Mol. Plant-Microbe Interact. 19*, 914−923.

(6) Lévy, J., Bres, C., Geurts, R., Chalhoub, B., Kulikova, O., Duc, G., Journet, E. P., Ané, J. M., Lauber, E., Bisseling, T., Dénarié, J., Rosenberg, C., and Debellé, F. (2004) A putative Ca^{2+} and calmodulin-dependent protein kinase required for bacterial and fungal symbioses. *Science 303*, 1361−1364.

(7) Mitra, R. M., Gleason, C. A., Edwards, A., Hadfield, J., Downie, J. A., Oldroyd, G. E., and Long, S. R. (2004) A Ca^{2+}/calmodulin-dependent protein kinase required for symbiotic nodule development: Gene identification by transcript-based cloning. *Proc. Natl. Acad. Sci. U.S.A. 101*, 4701−4705.

(8) Yano, K., Yoshida, S., Müller, J., Singh, S., Banba, M., Vickers, K., Markmann, K., White, C., Schuller, B., Sato, S., Asamizu, E., Tabata, S., Murooka, Y., Perry, J., Wang, T. L., Kawaguchi, M., Imaizumi-Anraku, H., Hayashi, M., and Parniske, M. (2008) CYCLOPS, a mediator of symbiotic intracellular accommodation. *Proc. Natl. Acad. Sci. U.S.A. 105*, 20540−20545.

(9) Tirichine, L., Imaizumi-Anraku, H., Yoshida, S., Murakami, Y., Madsen, L. H., Miwa, H., Nakagawa, T., Sandal, N., Albrektsen, A. S., Kawaguchi, M., Downie, A., Sato, S., Tabata, S., Kouchi, H., Parniske, M., Kawasaki, S., and Stougaard, J. (2006) Deregulation of a Ca^{2+}/calmodulin-dependent kinase leads to spontaneous nodule development. *Nature 441*, 1153−1156.

(10) Gleason, C., Chaudhuri, S., Yang, T., Munoz, A., Poovaiah, B. W., and Oldroyd, G. E. D. (2006) Nodulation independent of rhizobia induced by a calcium-activated kinase lacking autoinhibition. *Nature 441*, 1149−1152.

(11) Patil, S., Takezawa, D., and Poovaiah, B. W. (1995) Chimeric plant calcium/calmodulin-dependent protein kinase gene with a neural visinin-like calcium-binding domain. *Proc. Natl. Acad. Sci. U.S.A. 92*, 4897−4901.

(12) Ramachandiran, S., Takezawa, D., Wang, W., and Poovaiah, B. W. (1997) Functional domains of plant chimeric calcium/calmodulin-dependent protein kinase: Regulation by autoinhibitory and visinin-like domains. *J. Biochem. 121*, 984−990.

(13) Takezawa, D., Ramachandiran, S., Paranjape, V., and Poovaiah, B. W. (1996) Dual regulation of a chimeric plant serine/threonine kinase by calcium and calcium/calmodulin. *J. Biol. Chem. 271*, 8126−8132.

(14) Sathyanarayanan, P. V., Cremo, C. R., and Poovaiah, B. W. (2000) Plant chimeric Ca^{2+}/calmodulin-dependent protein kinase. Role of the neural visinin-like domain in regulating autophosphorylation and calmodulin affinity. *J. Biol. Chem. 275*, 30417−30422.

(15) Pandey, S., and Sopory, S. K. (2001) *Zea mays* CCaMK: Autophosphorylation-dependent substrate phosphorylation and down-regulation by red light. *J. Exp. Bot. 52*, 691−700.

(16) Shimoda, Y., Han, L., Yamazaki, T., Suzuki, R., Hayashi, M., and Imaizumi-Anraku, H. (2012) Rhizobial and fungal symbioses show different requirements for calmodulin binding to calcium calmodulin-dependent protein kinase in *Lotus japonicus*. *Plant Cell 24*, 304−321.

(17) Gifford, J. L., Walsh, M. P., and Vogel, H. J. (2007) Structures and metal-ion-binding properties of the Ca^{2+}-binding helix-loop-helix EF-hand motifs. *Biochem. J. 405*, 199−221.
(18) Studier, F. W. (2005) Protein production by auto-induction in high-density shaking cultures. *Protein Expression Purif. 41*, 207−234.
(19) Gasteiger, E., Hoogland, C., Gattiker, A., Duvaud, S., Wilkins, M. R., Appel, R. D., and Bairoch, A. (2005) Protein identification and analysis tools on the ExPASy server. In *The Proteomics Protocols Handbook* (Walker, J. M., Ed.) pp 571−607, Humana Press, Totowa, NJ.
(20) Fromm, H., and Chua, N. H. (1992) Cloning of plant cDNAs encoding calmodulin-binding proteins using ^{35}S-labeled recombinant calmodulin as a probe. *Plant Mol. Biol. Rep. 10*, 199−206.
(21) Demeler, B. (2005) UltraScan: A comprehensive data analysis software package for analytical ultracentrifugation experiments. In *Analytical Ultracentrifugation Techniques and Methods* (Scott, D. J., Harding, S. E., and Rowe, A. J., Eds.) pp 210−230, The Royal Society of Chemistry, Cambridge, U.K.
(22) Hu, P., Ye, Q.-Z., and Loo, J. A. (1994) Calcium stoichiometry determination for calcium binding proteins by electrospray ionization mass spectrometry. *Anal. Chem. 66*, 4190−4194.
(23) Shirran, S. L., and Barran, P. E. (2009) The use of ESI-MS to probe the binding of divalent cations to calmodulin. *J. Am. Soc. Mass Spectrom. 20*, 1159−1171.
(24) Bayley, P., Ahlstrom, P., Martin, S. R., and Forsen, S. (1984) The kinetics of calcium binding to calmodulin: Quin 2 and ANS stopped-flow fluorescence studies. *Biochem. Biophys. Res. Commun. 120*, 185−191.
(25) Whitmore, L., and Wallace, B. A. (2004) DICHROWEB, an online server for protein secondary structure analyses from circular dichroism spectroscopic data. *Nucleic Acids Res. 32*, W668−W673.
(26) Sreerama, N., and Woody, R. W. (2000) Estimation of protein secondary structure from circular dichroism spectra: Comparison of CONTIN, SELCON, and CDSSTR methods with an expanded reference set. *Anal. Biochem. 287*, 252−260.
(27) Peterson, B. Z., DeMaria, C. D., Adelman, J. P., and Yue, D. T. (1999) Calmodulin is the Ca^{2+} sensor for Ca^{2+}-dependent inactivation of L-type calcium channels. *Neuron 22*, 549−558.
(28) Putkey, J. A., Sweeney, H. L., and Campbell, S. T. (1989) Site-directed mutation of the trigger calcium-binding sites in cardiac troponin C. *J. Biol. Chem. 264*, 12370−12378.
(29) Venyaminov, S. Y., Klimtchuk, E. S., Bajzer, Z., and Craig, T. A. (2004) Changes in structure and stability of calbindin-D_{28K} upon calcium binding. *Anal. Biochem. 334*, 97−105.
(30) Rosenberg, O. S., Deindl, S., Sung, R. J., Nairn, A. C., and Kuriyan, J. (2005) Structure of the autoinhibited kinase domain of CaMKII and SAXS analysis of the holoenzyme. *Cell 123*, 849−860.
(31) Pain, R. (2001) *Determining the CD Spectrum of a Protein*, John Wiley & Sons, Inc., New York.
(32) Karley, A. J., and White, P. J. (2009) Moving cationic minerals to edible tissues: Potassium, magnesium, calcium. *Curr. Opin. Plant Biol. 12*, 291−298.
(33) Peersen, O. B., Madsen, T. S., and Falke, J. J. (1997) Intermolecular tuning of calmodulin by target peptides and proteins: Differential effects on Ca^{2+} binding and implications for kinase activation. *Protein Sci. 6*, 794−807.
(34) Burgoyne, R. D., and Weiss, J. L. (2001) The neuronal calcium sensor family of Ca^{2+}-binding proteins. *Biochem. J. 353*, 1−12.
(35) Kolukisaoglu, Ü., Weinl, S., Blazevic, D., Batistic, O., and Kudla, J. (2004) Calcium sensors and their interacting protein kinases: Genomics of the *Arabidopsis* and rice CBL-CIPK signaling networks. *Plant Physiol. 134*, 43−58.
(36) Wernimont, A. K., Artz, J. D., Finerty, P., Lin, Y. H., Amani, M., Allali-Hassani, A., Senisterra, G., Vedadi, M., Tempel, W., Mackenzie, F., Chau, I., Lourido, S., Sibley, L. D., and Hui, R. (2010) Structures of apicomplexan calcium-dependent protein kinases reveal mechanism of activation by calcium. *Nat. Struct. Mol. Biol. 17*, 596−601.
(37) Felle, H. H., Kondorosi, É., Kondorosi, Á., and Schultze, M. (1999) Elevation of the cytosolic free Ca^{2+} is indispensable for the transduction of the nod factor signal in alfalfa. *Plant Physiol. 121*, 273−279.
(38) De Koninck, P., and Schulman, H. (1998) Sensitivity of CaM kinase II to the frequency of Ca^{2+} oscillations. *Science 279*, 227−230.